Mass Spectrometry-Based Metabolite Profiling and Antioxidant Activity of *Aloe vera* (*Aloe barbadensis* Miller) in Different Growth Stages

Sarah Lee,[†] Seon-Gil Do,[§] Sun Yeou Kim,[⊥] Jinwan Kim,[§] Yoojeong Jin,[§] and Choong Hwan Lee*,[†]

[†]Division of Bioscience and Biotechnology, Konkuk University, Seoul 143-701, Republic of Korea
[§]Life Science Research Institute, Univera, Inc., Seoul 133-120, Republic of Korea
[⊥]College of Pharmacy, Gachon University, Incheon 406-70, Republic of Korea

S *Supporting Information*

ABSTRACT: Metabolite profiling of four different-sized *Aloe vera* plants was performed using gas chromatography−ion trap−mass spectrometry (GC-IT-MS) and ultra performance liquid chromatography−quadrupole−time of flight−mass spectrometry (UPLC-Q-TOF-MS) with multivariate analysis. Amino acids, sugars, and organic acids related to growth and development were identified by sizes. In particular, the relative contents of glucose, fructose, alanine, valine, and aspartic acid increased gradually as the size of the aloe increased. Anthraquinone derivatives such as 7-hydroxy-8-*O*-methylaloin, 7-hydroxyaloin A, and 6′-malonylnataloins A and B increased gradually, whereas chromone derivatives decreased continuously as the size of the aloe increased. The A30 aloe (size = 20−30 cm) with relatively high contents of aloins A and B, was suggested to have antioxidant components showing the highest antioxidant activity among the four different sizes of aloe. These data suggested that MS-based metabolomic approaches can illuminate metabolite changes associated with growth and development and can explain their change of antioxidant activity.

KEYWORDS: *Aloe vera, size, metabolite profiling, antioxidant activity, gas chromatography−ion trap−mass spectrometry (GC-IT-MS), ultra performance liquid chromatography−quadrupole−time of flight−mass spectrometry (UPLC-Q-TOF-MS)*

■ INTRODUCTION

The genus *Aloe* (Aloeaceae) has more than 360 different species cultivated in North America, Europe, and Asia. Among them, *Aloe vera* L. (*A. barbadensis* Miller) has long been used in health foods and cosmetic products.[1] *A. vera* gel and its products are commercially used for creams, yogurts, beverages, and desserts.[2,3]

Studies on biological activities such as antioxidant,[4] antidiabetic,[5] and antimicrobial effects[6] of *A. vera* extracts have been widely reported. Even the pharmacological functions for a wide range of human diseases, including cancer, AIDS, and ulcerative colitis, have been discussed.[7] Aloe extracts possess strong radical-scavenging activity,[8] and potent antioxidative compounds have been isolated.[9] In particular, the antioxidant activity of a variety of polyphenol compounds such as anthraquinones and chromones has been reported.[4]

Metabolomics techniques have been used to screen potential "biomarkers" in plants.[10] These techniques, along with multivariate data analyses, are playing an important role in many aspects of biomedical and phytochemical studies, including biomarker screening, quality control, bioactivity, toxicity, chemotaxonomy, and environmental metabolism.[11] Previous mass spectrometry (MS)-based metabolomic studies have illustrated that this technique can be effectively used for quality assessment of plants, including *Angelica acutiloba*,[12] *Arabidopsis thaliana*,[13] *Artemisia annua* L.,[14] and *Camellia sinensis*.[15,16]

In this study, we used gas chromatography−ion trap−mass spectrometry (GC-IT-MS) and ultra performance liquid chromatography−quadrupole−time of flight−mass spectrometry (UPLC-Q-TOF-MS) combined with multivariate analyses, including principal component analysis (PCA), partial least-squares discriminant analysis (PLS-DA), and orthogonal projection to latent structures discriminate analysis (OPLS-DA), for metabolic profiling of *A. vera*. The objective of this study was to characterize metabolic differences and to investigate changes of antioxidant activity of *A. vera* according to sample size as a biomarker related to growth and development.

■ MATERIALS AND METHODS

Chemicals and Reagents. Methanol, acetonitrile, and water were purchased from Fisher Scientific (Pittsburgh, PA, USA). Methoxyamine hydrochloride, *N*-methyl-*N*-(trimethylsilyl)trifluoroacetamide (MSTFA), gallic acid, potassium persulfate, 2,2″-azinobis(3-ethylbenzothiazoline-6-sulfonic acid) diammonium salt (ABTS), 1,1-diphenyl-2-picrylhydrazyl (DPPH), formic acid, pyridine, and standard compounds were obtained from Sigma Chemical Co. (St. Louis, MO, USA). All other chemicals used were of analytical grade.

Plant Materials. *A. vera* samples were cultivated on Jeju Island, South Korea (N 33° 20′ 36.62″, E 126° 46′ 11.63″). The greenhouse

was maintained at temperatures of approximately 15−35 °C. In the winter season, the temperature in the greenhouse did not drop below 15 °C. The soil was a well-drained loamy soil type. From spring to autumn, the greenhouse was opened to control the sunlight and humidity adequately. Samples were randomly sorted by morphology into four different sizes (lengths): A10, <10 cm; A20, 10−20 cm; A30, 20−30 cm; and A50, >50 cm. A50 was a mature sample commercially used in industry. They were pooled about 10−20 leaves per different-sized sample. The whole fresh leaves of the *A. vera* samples were washed and homogenized with a homogenizer (NUC Electronic, Seoul, Korea). They were freeze-dried over 5 days and stored at below −70 °C before extraction.

Sample Preparation. Dried sample (0.1 g) was extracted with 8 mL of methanol using a Twist Shaker (BioFree, Seoul, Korea) for 12 h. After extraction, the extract was centrifuged at 4 °C and 3000 rpm for 10 min (Hettich Zentrifugen, Universal 320) with a rotor consisting of six 50 mL centrifuge tubes. One milliliter of the supernatant was completely dried with a speed vacuum concentrator (Biotron, Seoul, Korea) for 12 h. Oximation and derivatization were performed for the GC-MS analysis. Fifty microliters of methoxyamine hydrochloride (20 mg/mL) in pyridine was added to the dried extract and oximated at 30 °C for 90 min. Then, the oximated samples were silylated with 50 µL of MSTFA at 37 °C for 30 min. Dried samples were resolved with methanol and filtered through a 0.2 µm PTFE filter for the UPLC-Q-TOF-MS analysis. Five analytical replications from each of the different-sized samples were used both GC-IT-MS and UPLC-Q-TOF-MS analyses.

GC-IT-MS Analysis. A Varian CP-3800 GC system equipped with a Varian CP-8400 autosampler was coupled with a Varian 4000 ion trap EI MS detector system (Varian, Palo Alto, CA, USA). A VF-1MS capillary column (30 m length × 0.25 mm i.d. × 0.25 µm film thickness) was used with helium at a constant flow of 1.0 mL/min. The oven temperature was held at 100 °C for 2 min, then ramped to 300 °C at a rate of 5 °C/min, and held for 10 min. The mass data collected in the EI mode with 70 eV ionization energy were used for full scan at m/z 50−1000. The injector and transfer line temperatures were 200 and 250 °C, respectively. The reaction mixtures were transferred to 2 mL GC autosampler vials, and 1 µL of reactant was injected into the GC-IT-MS with a split ratio of 25:1.

UPLC-Q-TOF-MS Analysis. UPLC was performed on a Waters Acquity UPLC system (Waters Corp., Milford, MA, USA) equipped with a binary solvent delivery system, an autosampler, and a UV detector. Chromatographic separation was performed on a Waters Acquity high-performance liquid chromatography (HPLC) BEH C$_{18}$ column (100 × 2.1 mm i.d. × 1.7 µm particle size). The elution was performed with an acetonitrile/water gradient containing 0.1% formic acid. The gradient was linearly increased from 0 to 90% acetonitrile in 12 min and then decreased to 0% over 3 min. Total run time, including re-equilibration of the column to the initial conditions, was 17 min. The injection volume was 5 µL, and the flow rate was 0.3 mL/min. The Waters Q-TOF Premier (Micromass MS Technologies, Manchester, UK) was operated in a wide-pass quadrupole mode for the MS experiments, and the TOF data were collected between m/z 100 and 1500 in negative (−) and positive (+) ion modes. The desolvation gas (nitrogen) was set to 600 L/h at a temperature of 200 °C; the cone gas (nitrogen) was set to 50 L/h, and the source temperature was 100 °C. The capillary and cone voltages were set to 3.0 kV and 40 V, respectively. Data were collected in the centroid mode, with a scan accumulation time of 0.2 s. All analyses were acquired using an independent reference spray via the LockSpray interference to ensure accuracy and reproducibility; leucine enkephalin ions were used as the lock mass (m/z 554.2615 (−) and 556.2771 (+)) at a flow rate of 10 µL/min. The accurate masses and compositions for the precursor ions and for the product ions were calculated using the MassLynx software (Waters Corp.) incorporated in the instrument. The Masslynx software has a feature that calculates all possible elemental compositions from the accurate mass. The MSn analysis was also performed under the same conditions used for metabolite full scanning. The final identification can then be

performed on the basis of accurate mass measurements of the parent ions and fragments obtained in the MS/MS experiments.

Data Processing and Multivariate Data Analysis. GC-IT-MS raw data were acquired with MS Workstation 6.9 software (Varian) and converted to netCDF format using Vx capture version 2.1 (Adron Systems, Laporte, MN, USA). Data preprocessing for the UPLC-Q-TOF-MS analysis was performed with MassLynx software, and raw data files were converted into netCDF (*.cdf) format with Waters DataBridge version 2.1 software. After conversion, the MS data were processed using the Metalign software package (http://www.metalign.nl) to obtain a data matrix containing retention times, accurate masses, and normalized peak intensities. The resulting data were exported to Excel (Microsoft, Redmond, WA, USA), and a statistical analysis was performed using SIMCA-P+ 12.0 software (Umetrics, Umea, Sweden). Unsupervised PCA and supervised PLS-DA were used to compare different sizes of *A. vera* samples and to identify the major metabolites by size. The data sets were UV scaled in a columnwise manner before PCA and PLS-DA modeling. Metabolites with the largest variable importance in the projection (VIP) values in the model were regarded as potential biomarkers. Metabolites with a VIP value >0.7 and a p value <0.05 were selected as suitable biomarkers. OPLS-DA was also performed to obtain information on differences in the metabolite composition of two (A10 and A30) samples. Variables were mean centered and scaled to pareto variance for OPLS-DA in a columnwise manner. Biomarkers for the difference between A10 and A30 were subsequently identified by analyzing the S-plot, which was declared with covariance (p) and correlation (pcorr). Significantly different metabolites were represented by box−whisker plots using Statistica, version 7.0 (StatSoft Inc., Tulsa, OK, USA), and differences in DPPH and ABTS radical-scavenging activities were tested by analysis of variance and Duncan's multiple-range test using SPSS version 12.0 software (SPSS Inc., Chicago, IL, USA).

Biomarker Identification. After the multivariate statistical analysis, major metabolites were positively identified using standard compounds by comparing both the mass spectra and retention time. When standard compounds were not available, a tentative identification was made on the basis of the MS spectra using the NIST05 MS Library (NIST, 2005), references, combined chemical dictionary version 7.2 (Chapman & Hall/CRC), and an in-house library.

Determination of Antioxidant Activities by ABTS and DPPH Free Radical-Scavenging Activity. The ABTS assay procedure followed the method of Re et al.[17] with some modifications. The stock solutions included 7 mM ABTS solution and 2.45 mM potassium persulfate solution. The working solution was then prepared by mixing the two stock solutions in equal quantities and allowing them to react for 12 h at room temperature in the dark. The solution was then diluted until the absorbance reached 0.7 ± 0.02 at 734 nm using a spectrophotometer (Spectronic Genesys 6, Thermo Electron, Madison, WI, USA). Each aloe extract (10 µL, 3 mg/mL) was reacted with 190 µL of the ABTS diluted solution for 7 min in the dark. Then, the absorbance was taken at 734 nm using a spectrophotometer. The standard curve was linear between 0.0625 and 1 mM Trolox equivalents. Results are expressed in millimolar Trolox equivalents (TE) per gram dry weight (dw). The DPPH assay was conducted according to the method of Dietz et al.[18] with some modifications. *A. vera* extracts (20 µL, 3 mg/mL) were reacted with a 180 µM DPPH ethanol solution for 20 min at room temperature. Then, the absorbance was taken at 515 nm. The standard curve was linear between 0.0625 and 1 mM Trolox equivalents. Experiments were carried out in triplicate. Antioxidant activities of aloin B, isoaloeresin D, and aloin A were also determined by the same methods. Results are expressed in millimolar Trolox equivalents (TE) per milligram dry weight (dw).

■ RESULTS AND DISCUSSION

Metabolite Profiling of Different Sizes of *A. vera* by GC-IT-MS and UPLC-Q-TOF-MS Analyses. Different sizes of aloe were subjected to metabolomics analysis by GC-IT-MS
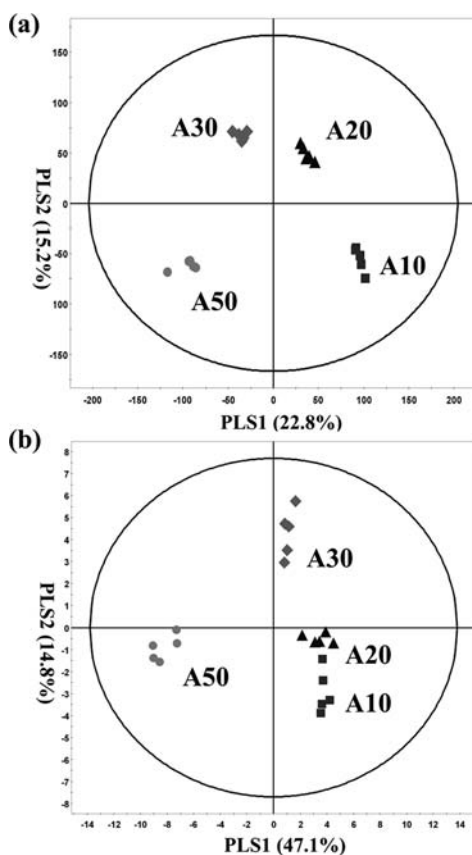
Figure 1. PLS-DA score plots analyzed by GC-IT-MS (a) and UPLC-Q-TOF-MS (b) of different sizes of aloe samples: A10, <10 cm; A20, 10−20 cm; A30, 20−30 cm; A50, >50 cm.

Table 1. Differential Metabolites Identified by GC-IT-MS Contributing to Differences in the Sizes of the Aloe Samples

RT[a] (min)	identified ion (m/z)[b]	metabolite[c]	derivatized[d]	ID[e]
4.4	116	alanine	$(TMS)_2$	MS/STD
5.8	144, 218	valine	$(TMS)_2$	MS/STD
6.8	147	succinic acid	$(TMS)_2$	MS/STD
6.9	148, 174, 248	arabitol	$(TMS)_5$	MS/STD
9.0	147	malic acid	$(TMS)_3$	MS/STD
9.3	156	pyroglutamic acid	$(TMS)_2$	MS/STD
9.4	147, 232	aspartic acid	$(TMS)_3$	MS/STD
9.6	174, 304	γ-aminobutyric acid (GABA)	$(TMS)_3$	MS/STD
11.2	148, 217	arabinose	$(TMS)_4$	MS/STD
13.5	217	fructose	MeOX $(TMS)_5$	MS/STD
13.7	148, 217	glucose	MeOX $(TMS)_5$	MS/STD
14.0	333	glucuronic acid	$(TMS)_5$	MS/STD
20.0	361	sucrose	$(TMS)_8$	MS/STD

[a]Retention time. [b]m/z values are the selected ion(s) for identification and quantification of individual derivatized metabolites. [c]Identified metabolites based on variable importance projection (VIP) analysis with cutoff value of 0.7 and a p value <0.05. [d]MEOX, methyloxime; TMS, trimethylsilyl. [e]Identification: MS, mass spectrum was consistent with those of NIST and in-house libraries; STD, mass spectrum was consistent with that of standard compound.

and UPLC-Q-TOF-MS. PCA, PLS-DA, and OPLS-DA were applied to the MS spectrum data to support pattern recognition and visualization of the metabolic differences in aloe samples according to the different sizes. The separation of different-sized aloe samples can be seen in the PLS-DA score plots from both the GC-IT-MS and UPLC-Q-TOF-MS data sets (Figure 1). Similar patterns were shown in the PCA (Supporting
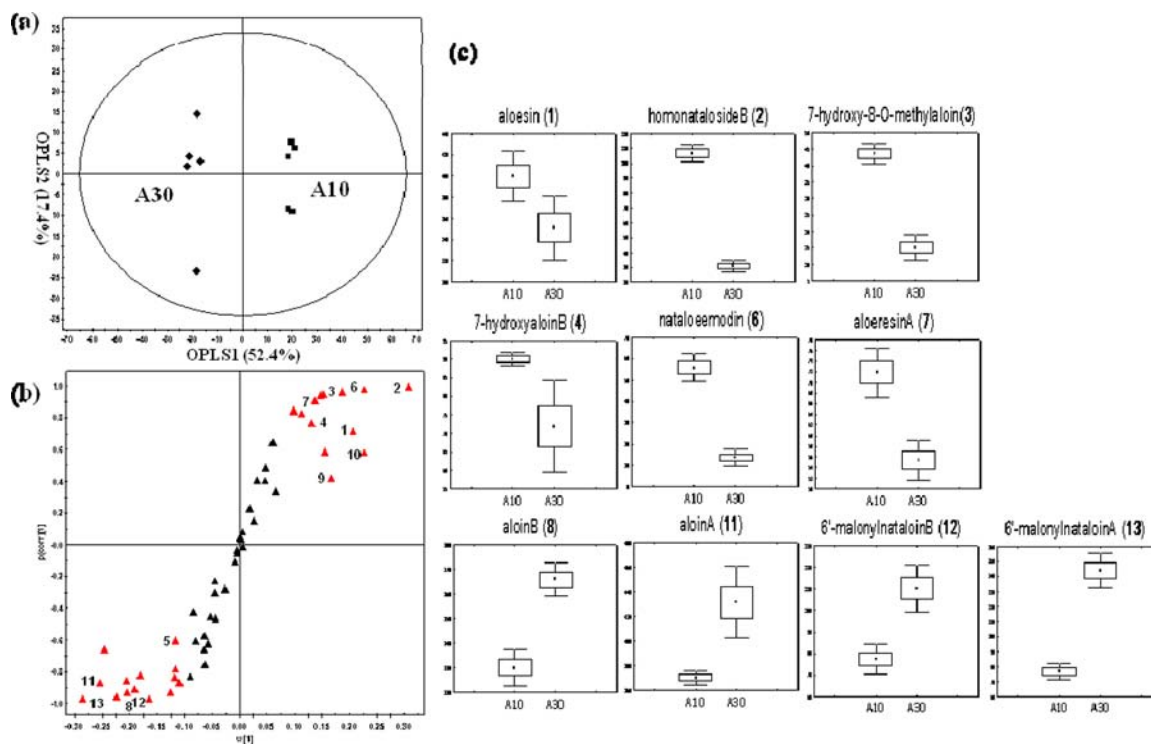

Figure 2. OPLS-DA score plot (a), S-plot (b), and box−whisker plots (c) analyzed by UPLC-Q-TOF-MS between the A10 and A30 samples (S-plot variable numbers are the same metabolite numbers shown in Table 2).

Table 2. Differential Metabolites Identified by UPLC-Q-TOF-MS Contributing to Differences in the Sizes of the Aloe Samples

RT^a (min)	$[M-H]^-$	MS^n fragment ions (m/z)	elemental composition	ppm	$iFit^b$ (norm)	difference^c (mDa)	putative metabolites^d	ID^e
3.26	393.1191	393 > 273, 245	$C_{19}H_{22}O_9$	1.3	2.4	0.5	aloesin (**1**)	STD/Ref[33,34]
4.66	593.1308	593 > 473, 431, 341, 311	$C_{28}H_{34}O_{14}$	3.2	2.6	1.9	homonataloside B (**2**)	Ref[35]
5.13	447.1291	447 > 327, 312, 284, 269, 265	$C_{22}H_{24}O_{10}$	3.8	1.7	1.7	7-hydroxy-8-O-methylaloin (**3**)	Ref[33]
5.34	433.1125	433 > 313, 270	$C_{21}H_{22}O_{10}$	−2.3	1.6	−1.0	7-hydroxyaloin B (**4**)	Ref[33]
5.45	433.1131	433 > 313, 270	$C_{21}H_{22}O_{10}$	−0.9	2.0	−0.4	7-hydroxyaloin A (**5**)	Ref[33]
5.62	431.0973	431 > 304, 174	$C_{21}H_{20}O_{10}$	−1.2	1.3	−0.5	nataloeemodin (**6**)	Ref[36]
6.42	539.1552	539 > 393, 375, 273, 231	$C_{28}H_{28}O_{11}$	−0.2	1.8	−0.1	aloeresinA (**7**)	Ref[33,34]
7.42	417.1182	417 > 298, 297	$C_{21}H_{22}O_9$	−1.0	1.0	−0.4	aloinB (**8**)	STD/Ref[33,37]
7.54	555.1863	555 > 297, 257, 243	$C_{29}H_{32}O_{11}$	−0.5	1.8	−0.3	isoaloeresin D (**9**)	Ref[26,33]
7.77	553.1710	553 > 408, 407	$C_{29}H_{30}O_{11}$	0.0	2.4	0.0	7-O-methylaloeresin A (**10**)	Ref[26]
7.85	417.1187	417 > 298, 297	$C_{21}H_{22}O_9$	0.2	1.8	0.1	aloin A (**11**)	STD/Ref[33,37]
8.06	459.1326^f	459, 297, 175	$C_{24}H_{24}O_{12}$	−2.4	1.2	−1.2	6′-malonylnataloin B (**12**)	Ref[28]
8.40	459.1326^f	459, 297, 175	$C_{24}H_{24}O_{12}$	−2.4	1.2	−1.2	6′-malonylnataloin A (**13**)	Ref[28]

^{a}Retention time. ^{b}iFit is a measure of how well the observed isotope pattern matches the predicted isotope pattern for the formula on that line. The lower the score, the better the fit. ^{c}Differences between observed mass and calculated mass. mDa stands for error in milliDaltons. ^{d}Identified metabolites based on variable importance projection (VIP) analysis with cutoff value of 0.7 and a p-value <0.05. ^{e}Identification: STD, standard compound/Ref, references. $^f[M-H-CO_2]^-$.
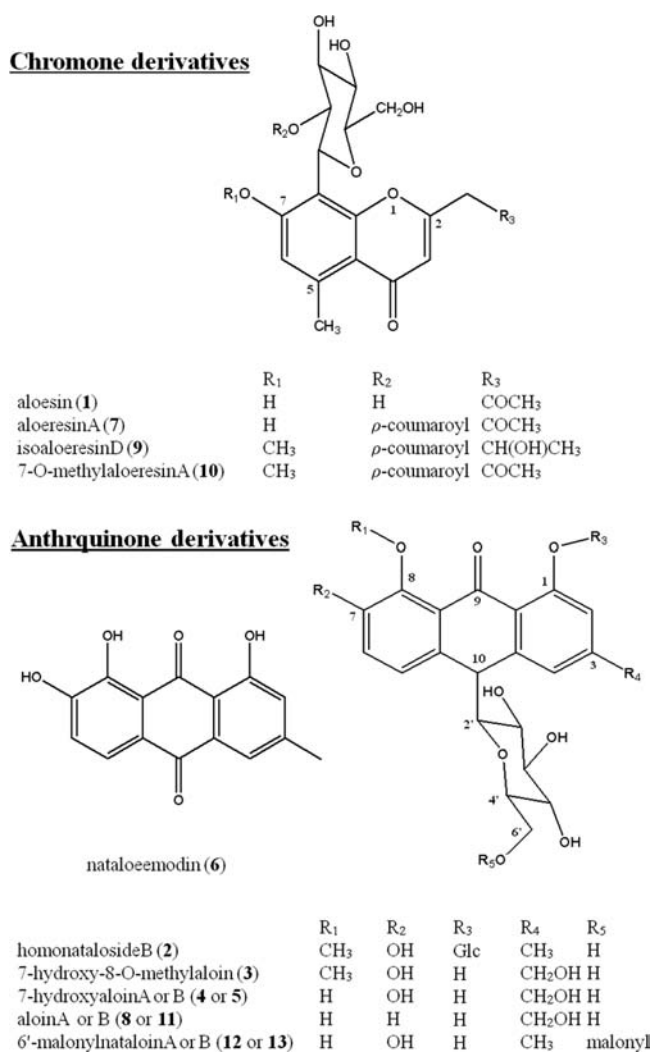

Figure 3. Structures of significantly different metabolites analyzed by UPLC-Q-TOF-MS in different sizes of aloe samples.

Information, Figure 1S). Additionally, OPLS-DA was performed on the UPLC-Q-TOF-MS data sets to predict the

differential metabolite composition between the A10 and A30 samples (Figure 2).

In the GC-IT-MS analysis, the PLS-DA score plot distinguished the different-sized aloe samples, indicating that primary metabolites related to growth and development were influenced by plant size. As shown in Figure 1a, the score plot explained 38.0% of the total variability. Small-sized aloe samples (A10 and A20, <20 cm) were separated from larger sizes (A30 and A50, >30 cm) along PLS1, whereas A10 and A50 (negative PLS2 dimension) were separated from A20 and A30 (positive PLS2 dimension) along PLS2. In Table 1, 13 metabolites were selected as differential variables using VIP values (VIP > 0.7) and p values (p < 0.05). Thirteen metabolites, including alanine, valine, succinic acid, arabitol, malic acid, pyroglutamic acid, aspartic acid, γ-aminobutyric acid (GABA), arabinose, fructose, glucose, glucuronic acid, and sucrose, were identified and confirmed using reference standards. In general, sugars, amino acids, and organic acids are the major energy source for photosynthesis and respiration in plants.[19] Sugars, as a carbon source, provide the energy required for growth and development of plants, and amino acids, as a nitrogen source, promote rapid growth along with an increase in leaf size.[20] In this study, the relative contents of sugars such as glucose and fructose and amino acids such as alanine, valine, and aspartic acid increased gradually as aloe size increased. These metabolites may be related to changes in sample size according to growth and development in aloe samples (Supporting Information, Figure 2S).

As Figure 1b for the UPLC-Q-TOF-MS analysis shows, A50 and other sized aloe samples were clearly separated by PLS1 (47.1%), and A30 and others were discriminated by PLS2 (14.8%). Thirteen secondary metabolites such as aloesin (**1**), homonataloside B (**2**), 7-hydroxy-8-O-methylaloin (**3**), 7-hydroxyaloin B (**4**), 7-hydroxyaloin A (**5**), nataloeemodin (**6**), aloeresin A (**7**), aloin B (**8**), isoaloeresin D (**9**), 7-O-methylaloeresin A (**10**), aloin A (**11**), 6′-malonylnataloin B (**12**), and 6′-malonylnataloin A (**13**) were significant metabolites for separating aloe samples by size (Table 2). OPLS-DA was subsequently applied to the UPLC-Q-TOF-MS data set to identify the significantly different metabolites separated by PLS2 in the PLS-DA analysis and to predict the
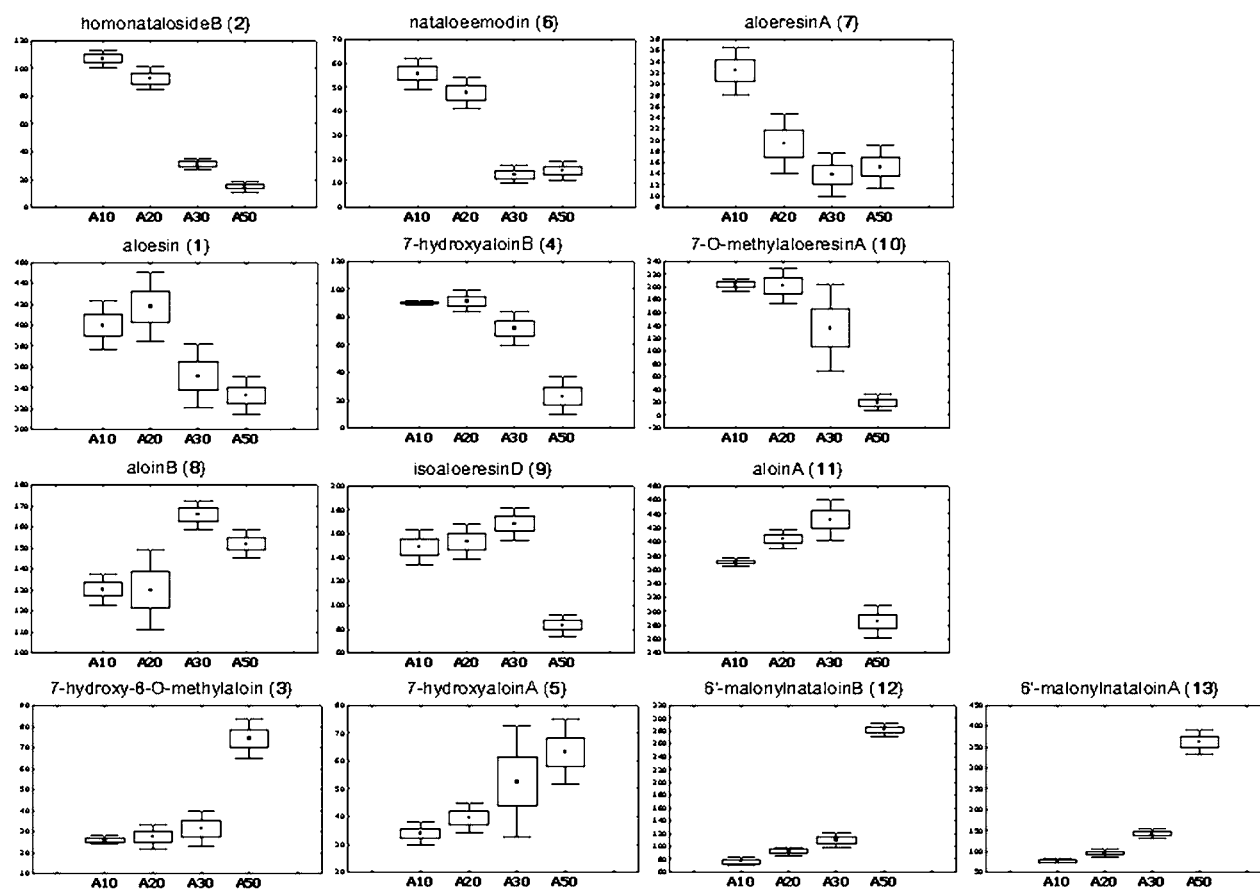
Figure 4. Box and whisker plots of significantly different metabolites analyzed by UPLC-Q-TOF-MS in different sizes of aloe samples. These metabolites were responsible for the differentiation in the PLS-DA model, VIP > 0.7 and $p < 0.05$ (line, mean; box, standard error; whisker, standard deviation).
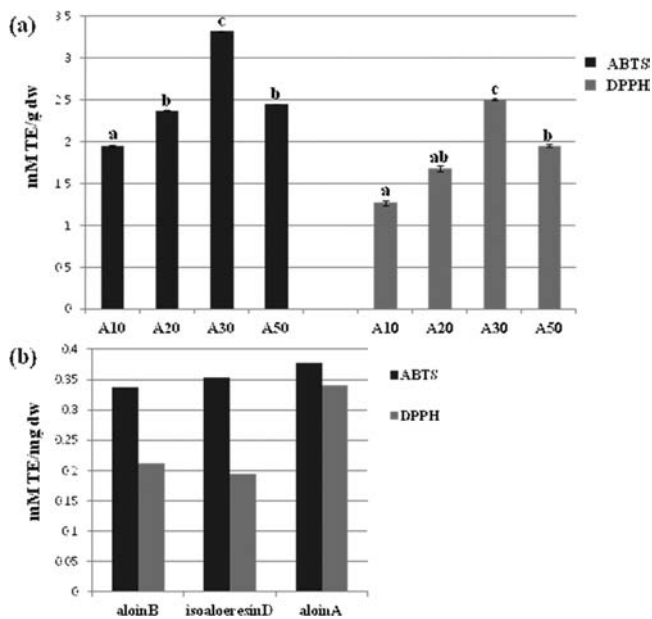

Figure 5. Antioxidant capacity of different sized aloe samples (mM Trolox equiv/g dw) (a) and antioxidant compounds (mM Trolox equiv/mg dw) (b) by ABTS and DPPH radical-scavenging activities. Different letters are significantly different by Duncan's multiple-range test following an analysis of variance ($P < 0.05$).

metabolites related to antioxidant activity. As shown in Figure 2, the score plot and S-plot showed the separation of A10 and A30 along the discriminating OPLS1 with $R^2 = 0.993$ and $Q^2 = 0.969$. The loading S-plot (Figure 2b) and box−whisker plot (Figure 2c) revealed that aloesin (**1**), homonataloside B (**2**), 7-hydroxy-8-*O*-methylaloin (**3**), nataloeemodin (**6**), aloeresin A (**7**), isoaloeresin D (**9**), and 7-*O*-methylaloeresin A (**10**) were related to A10, whereas aloin B (**8**), aloin A (**11**), 6′-malonylnataloin B (**12**), and 6′-malonylnataloin A (**13**) contributed to A30.

Major metabolites separated by aloe sample size mainly fell into two groups of anthraquinones and chromones (Figure 3). They were produced by the chalcone synthase (CHS) superfamily of type III polyketide synthase.[21] In particular, pentaketide chromone synthase (PCS) and octaketide synthase (OKS) were reported as main key enzymes to generate aromatic polyketides including anthraquinones and chromones.[21] Anthraquinones are tricyclic aromatic quinones with yellow, orange, and red colors,[22] and their derivatives modified by the addition of a sugar molecule have been recognized for their systematic significance in aloe species.[23,24] Aloin is a representative anthraquinone glycoside compound reported in most aloe species.[25] It is a mixture of two diastereoisomers, termed aloin A (also called barbaloin) and aloin B (or isobarbaloin), which have similar chemical properties.[25] Homonataloside B (**2**), 7-hydroxy-8-*O*-methylaloin (**3**), 7-hydroxyaloin B (**4**), 7-hydroxyaloin A (**5**), aloin B (**8**), aloin A (**11**), 6′-malonylnataloin B (**12**), and 6′-malonylnataloin A

(**13**) were also aloin derivatives with added functional groups. The other main metabolites to discriminate the size of aloe samples were chromone derivatives such as aloesin (**1**), aloeresin A (**7**), isoaloeresin D (**9**), and 7-*O*-methylaloeresin A (**10**). Aloeresin has a number of different isomers, which is interesting from a scientific and applied point of view.[26] As shown in Figure 4, chromones such as aloesin (**1**), aloeresin A (**7**), and 7-*O*-methylaloeresin A (**10**) were mainly related to small aloe samples (A10 and A20). Anthraquinone derivatives such as 7-hydroxy-8-*O*-methylaloin (**3**), 7-hydroxyaloin A (**5**), 6′-malonylnataloin B (**12**), and 6′-malonylnataloin A (**13**), were found at higher levels in A50 and gradually increased as aloe size increased. 6′-Malonylnataloin, a malonylated derivative of the anthrone nataloin, was a significant metabolite representing the A50 sample and separated by PLS1. As shown in Table 2, this metabolite was identified by the m/z values at 459 $[M - H - CO_2]^-$ due to the presence of a free carboxylic acid in the negative mode. It was previously detected in an East African species by HPLC−photodiode array analysis[27] and has been reported as a putative phytochemical biomarker for the East African taxa of maculate species.[28] The relative contents of 7-hydroxy-8-*O*-methylaloin A (**3**), 6′-malonylnataloin B (**12**), and 6′-malonylnataloin A (**13**) increased drastically, whereas 7-hydroxyaloin B (**4**), 7-*O*-methylaloeresin A (**10**), isoaloeresin D (**9**), and aloin A (**11**) decreased sharply between A30 and A50. This result suggests that further study of *A. vera* according to gradual growth and development is required to understand the sudden changes in metabolites.

Antioxidant Activity and Related Metabolites in Different Sizes of *A. vera* in the UPLC-Q-TOF-MS Analysis. DPPH and ABTS antioxidant activities are shown in Figure 5. The radical-scavenging activities of aloe extracts that can be measured as decolorizing activity following the trapping of the unpaired election were used to assess antioxidant capacity. On the basis of similar results from the two assays, the antioxidant activity of the aloe extracts followed the order A30 > A50 > A20 > A10 (Figure 5a). In both assays, A30 showed the highest antioxidant activity among the different sizes of aloe, suggesting that aloe of various sizes contains different active components and possesses different amounts of antioxidant activity. Hu et al. explained that polysaccharide and flavonoid contents of *A. vera* in different development stages were related to antioxidant activity.[29] According to some studies, phenolic metabolites such as anthraquinones and chromones are the main antioxidant compounds in various aloe species.[30,31] Anthraquinones such as aloin and its derivatives are potent antioxidants, and their antioxidant effect is dose-dependent.[32] In particular, aloin A is the main pharmacologically active compound obtained from *Aloe* species.[31] As an antioxidant, chromones such as aloesin, aloeresin A, and isoaloeresin D also have radical-scavenging activity.[23] As shown in Figure 4, relatively high contents of aloin B (**8**), isoaloeresin D (**9**), and aloin A (**11**) were found in the A30 sample. These compounds were measured for antioxidant activity (Figure 5b). In particular, the antioxidant activity of aloin A was higher than that of the other compounds in both ABTS and DPPH assays. It is speculated that different active components in different-sized aloe samples resulted in their various antioxidant activities. More studies are needed to clarify the antioxidant mechanisms of the aloe constituents and the effect of the growth period on aloe antioxidant activity.

■ ASSOCIATED CONTENT

Ⓢ Supporting Information

Figures of PCA score plots analyzed by GC-IT-MS and UPLC-Q-TOF-MS and box and whisker plots of significantly different metabolites analyzed by GC-IT-MS of different sizes of aloe samples. This material is available free of charge via the Internet at http://pubs.acs.org.

■ AUTHOR INFORMATION

Corresponding Author

*Phone: + 82-2-2049-6177. Fax: + 82-2-455-4291. E-mail: chlee123@konkuk.ac.kr.

Notes

The authors declare no competing financial interest.

■ REFERENCES

(1) Grindlay, D.; Reynolds, T. The *Aloe vera* phenomenon: areview of the properties and modern uses of the leaf parenchyma gel. *J. Ethnopharmacol.* **1986**, *16*, 117−151.

(2) Gutterman, Y.; Chauser-Volfson, E. The content of secondary phenol metabolites in pruned leaves of *Aloe arborescens*, comparison between two methods: leaf exudates and leaf water extract. *J. Nat. Med.* **2008**, *62*, 430−435.

(3) Reynolds, T. *Aloes: the Gnus Aloe*; CRC Press: Boca Raton, FL, 2004.

(4) Zonta, F.; Bogoni, P.; Masotti, P.; Micali, G. High-performance liquid chromatographic profiles of aloe constituents and determination of aloin in beverages, with reference to the EEC regulation for flavouring substances. *J. Chromatogr., A* **1995**, *718*, 99−106.

(5) Misawa, E.; Tanaka, M.; Nomaguchi, K.; Nabeshima, K.; Yamada, M.; Toida, T.; Iwatsuki, K. Oral ingestion of *Aloe vera* phytosterols alters hepatic gene expression profiles and ameliorates obesity-associated metabolic disorders in Zucker diabetic fatty rats. *J. Agric. Food Chem.* **2012**, *60*, 2799−2806.

(6) Ndhlala, A. R.; Amoo, S. O.; Stafford, G. I.; Finnie, J. F.; Van Staden, J. Antimicrobial, anti-inflammatory and mutagenic investigation of the South African tree aloe (*Aloe barberae*). *J. Ethnopharmacol.* **2009**, *124*, 404−408.

(7) Capasso, F.; Borrelli, F.; Capasso, R.; Carlo, G. D.; Izzo, A. A.; Pinto, L.; Mascolo, N.; Castaldo, S.; Longo, R. Aloe and its therapeutic use. *Phytother. Res.* **1998**, *12*, S124−S127.

(8) Zhang, Z. T.; Du, Y. J.; Liu, Q. G.; Liu, Y. Determination of the antioxidative effect of *Aloe vera*. *Nat. Prod. Res. Dev.* **2001**, *13*, 45−46.

(9) Lee, K. Y.; Weintraub, S. T.; Yu, B. P. Isolation and identification of a phenolic antioxidant from *Aloe barbadensis*. *Free Radical Biol. Med.* **2000**, *28*, 261−265.

(10) Van der Kooy, F.; Maltese, F.; Choi, Y. H.; Kim, H. K.; Verpoorte, R. Quality control of herbal material and phytopharmaceuticals with MS and NMR based metabolic fingerprinting. *Planta Med.* **2009**, *75*, 763−775.

(11) Liu, N. Q.; Cao, M.; Frédérich, M.; Choi, Y. H.; Verpoorte, R.; van der Kooy, F. Metabolomic investigation of the ethnopharmacological use of *Artemisia afra* with NMR spectroscopy and multivariate data analysis. *J. Ethnopharmacol.* **2010**, *128*, 230−235.

(12) Tianniam, S.; Tarachiwin, L.; Bamba, T.; Kobayashi, A.; Fukusaki, E. Metabolic profiling of *Angelica acutiloba* roots utilizing gas chromatography-time of-flight-mass spectrometry for quality assessment based on cultivation area and cultivar via multivariate pattern recognition. *J. Biosci. Bioeng.* **2008**, *105*, 655−659.

(13) t'Kindt, R.; Morreel, K.; Deforce, D.; Boerjan, W.; Bocxlaer, J. V. Joint GC-MS and LC-MS platforms for comprehensive plant metabolomics: repeatability and sample pre-treatment. *J. Chromatogr., B* 2009, *877*, 3572−3580.

(14) Ma, C. F.; Wang, H. H.; Lu, X.; Xu, G. W.; Liu, B. Y. Metabolic fingerprinting investigation of *Artemisia annua* L. in different stages of development by gas chromatography and gas chromatography-mass spectrometry. *J. Chromatogr., A* 2008, *1186*, 412−419.

(15) Ku, K. M.; Choi, J. N.; Kim, J.; Kim, J. K.; Yoo, L. G.; Jun Lee, S.; Hong, Y.-S.; Lee, C. H. Metabolomics analysis reveals the compositional differences of shade grown tea (*Camellia sinensis* L.). *J. Agric. Food Chem.* 2010, *58*, 418−426.

(16) Pongsuwan, W.; Bamba, T.; Harada, K.; Yonetani, T.; Kobayashi, A.; Fukusaki, E. High-throughput technique for comprehensive analysis of Japanese green tea quality assessment using ultraperformance liquid chromatography with time-of-flight mass spectrometry (UPLC/TOF MS). *J. Agric. Food Chem.* 2008, *56*, 10705−10708.

(17) Re, R.; Pellegrini, N.; Proteggente, A.; Pannala, A.; Yang, M.; Rice-Evans, C. Antioxidant activity applying an improved ABTS radical cation decolorization assay. *Free Radical Biol. Med.* 1999, *26*, 1231−1237.

(18) Dietz, B. M.; Kang, Y. H.; Liu, G.; Eggler, A. L.; Yao, P.; Chadwick, L. R.; Pauli, G. F.; Farnsworth, N. R.; Mesecar, A. D.; van Breemen, R. B.; Bolton, J. L. Xanthohumol isolated from *Humulus lupulus* inhibits menadione-induced DNA damage through induction of quinone reductase. *Chem. Res. Toxicol.* 2005, *18*, 1296−1305.

(19) Chen, S.; Hajirezaei, M.; Peisker, M.; Tschiersch, H.; Sonnewald, U.; Bornke, F. Decreased sucrose-6-phosphate phosphatase level in transgenic tobacco inhibits photosynthesis, alters carbohydrate partitioning, and reduces growth. *Planta* 2005, *221*, 479−492.

(20) Huston, M.; Smith, T. Plant succession: life history and competition. *Am. Nat.* 1987, *130*, 168−198.

(21) Abe, I. Engineering of plant polyketide biosynthesis. *Chem. Pharm. Bull.* 2008, *56*, 1505−1514.

(22) Izhaki, I. Emodin − a secondary metabolite with multiple ecological functions in higher plants. *New Phytol.* 2002, *155*, 205−217.

(23) Yagi, A.; Kabash, A.; Okamura, N.; Haraguchi, H.; Moustafa, S. M.; Khalifa, T. I. Antioxidant, free radical scavenging and antiinflammatory effects of aloesin derivatives in aloe vera. *Planta Med.* 2002, *68*, 957−960.

(24) Reynolds, T.; Dweck, A. C. *Aloe vera* leaf gel: a review update. *J. Ethnopharmacol.* 1999, *68*, 3−37.

(25) Okamura, N.; Asai, M.; Hine, N.; Yagi, A. High-performance liquid chromatographic determination of phenolic compounds in *Aloe* species. *J. Chromatogr., A* 1996, *746*, 225−231.

(26) Speranza, G.; Dadà, G.; Lunazzi, L.; Gramatica, P.; Manitto, P. A *C*-glucosylated 5-methylchromone from Kenya aloe. *Phytochemistry* 1986, *25*, 2219−2222.

(27) Wabuyele, E. *Studies on Eastern African aloes: aspects of taxonomy, conservation and ethnobotany*. Ph.D. Dissertation, University of Oslo, 2006.

(28) Grace, O. M.; Kokubun, T.; Veitch, N. C.; Simmonds, M. S. J. Characterisation of a nataloin derivative from *Aloe ellenbeckii*, a maculate species from east Africa. *S. Afr. J. Bot.* 2008, *74*, 761−763.

(29) Hu, Y.; Xu, J.; Hu, Q. Evaluation of antioxidant potential of aloe vera (*Aloe barbadensis* Miller) extracts. *J. Agric. Food Chem.* 2003, *51*, 7788−7791.

(30) Choi, S.; Chung, M.-H. A review on the relationship between aloe vera components and their biologic effects. *Semin. Integr. Med.* 2003, *1*, 53−62.

(31) Yuko, A.; Toshihiko, H.; Asuka, N.; Kenji, Y. Development of crude drug analysis by liquid chromatography, and UV and MS spectrometers. *J. Liq. Chromatogr.* 1990, *13*, 2449−2464.

(32) Tian, B.; Hua, Y. Concentration-dependence of prooxidant and antioxidant effects of aloin and aloe-emodin on DNA. *Food Chem.* 2005, *91*, 413−418.

(33) Fanali, S.; Aturki, Z.; D'Orazio, G.; Rocco, A.; Ferranti, A.; Mercolini, L.; Raggi, M. A. Analysis of aloe-based phytotherapeutic products by using nano-LC-MS. *J. Sep. Sci.* 2010, *33*, 2663−2670.

(34) Dell'Agri, M.; Giavarini, F.; Ferraboschi, P.; Galli, G.; Bosisio, E. Determination of aloesin and aloeresin A for the detection of aloe in beverages. *J. Agric. Food Chem.* 2007, *55*, 3363−3367.

(35) Viljoen, A. M.; Van Wyk, B.-E.; Van Heerd, F. R. The chemotaxonomic value of the diglucoside anthrone homonataloside B in the genus *Aloe*. *Biochem. Syst. Ecol.* 2002, *30*, 35−43.

(36) Dagne, E.; Bisrat, D.; Viljoen, A.; Van Wyk, B.-E. Chemistry of *Aloe* species. *Curr. Org. Chem.* 2000, *4*, 1055−1078.

(37) Waihenya, R.; Oliver, K.; Hansjörg, H.; Karl-H, Z.; Mtambo, M.; Nkwengulila, G. The phytochemical profile and identification of main phenolic compounds from the leaf. *Phytochem. Anal.* 2003, *14*, 83−86.